

UNIOSUN Journal of Engineering and Environmental Sciences. Vol. 1, No. 2. Sept. 2019

DOI: 10.36108/ujees/9102.10.0250

Comparative Analysis of the Adsorption of Methylene Blue Using Magnetised and Non-Magnetised Coconut Shell Biochar

Musa, A., Sani, B.S., Ibrahim, F.B. and Giwa, A.

Abstract: It is envisaged that magnetisation might alter the sorption behaviours of magnetised biochars due to some variation in the physicochemical properties from their precursor. This study evaluated the adsorption behaviours of a coconut shell biochar produced at 600 °C, CSB600, and its magnetised pair, MCSB600, in the adsorption of methylene blue (MB) from aqueous solutions. Langmuir, Freundlich and Redlich-Peterson isotherm models were used to describe the experimental isotherm using linear and nonlinear regression methods to determine the best fit for MB adsorption from the batch experiments conducted. The Langmuir model proved to be the best fit to explain the experimental data as it had the highest R² (0.9684 and 0.9855) from linear regression and the lowest hybrid fractional error function, HYBRID (4.58, 1.145) and marquardt's percent standard deviation, MPSD (10.61, 5.04) error function values from the nonlinear regression methods with maximum monolayer adsorption capacities of 5.590 and 5.229 mg/g for CSB600 and MCSB600 respectively. The magnetised biochar exhibited similar adsorption characteristics to what was observed for the non-magnetised biochar and only about 6.46% lower MB adsorption capacity was recorded. A p-value of 0.088 obtained suggested the isotherms were similar and therefore, magnetisation did not affect the adsorption of MB.

Keywords: Adsorption, Biochar, Methylene blue, Isotherm, Magnetised biochar

I. Introduction

Huge volumes of coloured wastewaters are generated [1, 2] by industries such as textile, paper, leather, plastics, food and cosmetics [3, 4] due to the wide application of dyes in these industries [2, 5, 6]. Treatment of wastewater is a challenging task for Environmental Engineers [7] and one of the most difficult requirements faced by industries is the removal of colour from wastewater [4, 8].

Musa, A. (Department of Civil Engineering Technology, The Federal Polytechnic, Nasarawa, Nigeria.)

Sani, B.S., Ibrahim, F.B. (Department of Water Resources & Environmental Engineering, Ahmadu Bello University, Zaria, Nigeria)

Giwa, A (Department of Polymer & Textile Engineering, Ahmadu Bello University, Zaria, Nigeria)

Corresponding author: <u>abdulmalikmusa44@gmail.com</u> Phone Number: +2347034655806 Dye loaded wastewater results in major environmental problems and their treatment is not only difficult [8] but hardly achieved through conventional wastewater treatments [9]. However, adsorption process has proved to be a suitable option [4, 10] for the treatment of dye loaded wastewater due its simplicity, ease of operation [11], slight maintenance requirement, comparatively cheap [12], produces the least sludge and the possibility of access to low cost adsorbents [13].

Methylene blue (MB) is a cationic dye, the most commonly used dye for colouring among all other dyes of its category [3] and has the molecular formula, C₁₆H₁₈N₃SCI. It exists as a dark green crystalline powder which is odourless, stable in air and forms deep blue solution in water or alcohol [14]. Its structure and properties are presented in Figure 1 and Table 1.

MB dissociates in aqueous solution as electrolytes into methylene blue cation [15] and chloride ion; with several adsorbents able to retain the cation [16]. In humans, MB causes increase heart rate, vomiting, shock, Heinz body formation, cyanosis, jaundice, quadriplegia, and tissue necrosis [5] respectively.

Figure 1: Structure of methylene blue

Table 1: Properties of methylene blue

Properties	Methylene Blue
Molecular formula	$C_{16}H_{18}N_3SCI$
Melting Point	100 - 110 °C
Density (g/ml)	1.0 (20 °C)
Vapour Pressure (mmHg)	1.30X10 ⁻⁷ (25 °C)
Molecular mass (g/mol)	319.85
Solubility (g/L)	43.6 in Water (25 °C)
Maximum wavelength (nm)	664

The separation of powdered carbon from cleaned environmental matrices has been a challenge but magnetised biochars (MBC) have been envisaged to be an alternative route to the separation of pollutant loaded sorbents from cleaned environmental matrices [17]. Fine sized magnetic sorbents can be readily separated from treated wastewater [18] using some magnetic separation techniques even if the solution contains a significant concentration of solids [19].

MBCs produced through wet co-precipitation [4, 17, 20-25] is an efficient method to enable the sorbent to be effectively separated by magnetic separation [26]. However, MBCs have higher production costs, and their properties often

change in comparison with their pristine biochars [17] which may affect its sorption performance. Therefore, the sorption behaviours of the pristine biochar may not be the same in comparison with its magnetised pair. Understanding of possible trade-offs between the desire of magnetisation and its potential side-effects on the sorption properties of magnetic sorbents is also required in order to properly assess its economic value [17].

The aim of this study was to evaluate and compare the methylene blue adsorption properties of coconut shell biochars and magnetised coconut shell biochar through sorption isotherms.

II. Materials and Methods

A. Adsorbents

Two biochars, CSB600 and MCSB600 that were produced through carbonisation at 600 °C and magnetisation by chemical wet co-precipitation method respectively were used as the adsorbents. The MCSB600 is the magnetised pair produced from its pristine biochar, CSB600.

B. Adsorbate

Methylene blue (MB) also known as Methylthionine Chloride was obtained from BDH Chemicals, England, with 99.9% purity. A 500 mg/l standard solution was prepared by dissolving accurate quantity of MB in a volumetric flask containing 1000 ml of distilled water and agitated vigorously. 50 ml of the adsorbate working solutions (9-45 mg/l) were made in triplicates from the stock solution by dilution into screw capped 120 ml vials.

C. Adsorption Capacity Test

About 100 mg of CSB600 and MCS600 were accurately weighed in a balance (AX224/E,

Ohaus Adventurer, USA) and placed into vials in duplicate which contain the 50 ml MB solutions. Separate vials contain MB solutions without the biochars, which served as the control and were subjected to equal treatments. Both samples were shaken at 130 rpm for 4 hours in a shaker (Techmel TT 12F) and immediately filtered using a Whatman No.1 filter paper.

The absorbance of all the samples was measured using a UV-visible Spectrophotometer (Cary Series, Agilent) at the maximum absorbance wavelength of 664 nm with their concentrations obtained from the calibration curve. The obtained concentrations 3.70, 12.50, 26.60 and 32.70 mg/l from the control sample were considered as the initial concentrations (Co). The equilibrium concentrations, C_e was the average concentrations from the adsorbent/adsorbate duplicated samples.

The adsorption equilibrium, *Qe* (mg/g) and percentage adsorption, *R* (%) were calculated using equations 1 and 2 respectively.

$$Qe = \frac{(co - c_e)}{m} * V \tag{1}$$

$$R = \frac{(Co - C_e)}{Co} * 100 \tag{2}$$

where Co and Ce (mg/l) are the initial and equilibrium liquid phase sorbate concentration of the adsorbate (MB dye); m is the mass of adsorbent used (g); V is the volume of adsorbate solution used (ml).

D. Adsorption Isotherm Models

The Langmuir, Freundlich and Redlich-Peterson isotherm models were considered to model the sorption system. Linear and nonlinear regression methods were employed to determine the isotherm model parameters.

i. Linear Regression Methods

(a) Langmuir isotherm

The Langmuir isotherm [27] model is given in equation 3. It assumes monolayer adsorption over a surface that is homogenous where adsorption can only occur at a fixed number of identical sites [28].

$$Q_e = \frac{Q_m K_L C_e}{1 + K_L C_e} \tag{3}$$

The Linear Transformed (LTF) Langmuir-type 1 (LANG-L1) and Langmuir-type 2 (LANGL-L2) models were used to analyse the equilibrium data and are expressed in equations 4 and 5 respectively.

$$\frac{C_e}{Qe} = \frac{1}{Q_{m1K_{L1}}} + \frac{C_e}{Q_{m1}} \tag{4}$$

A plot of $\frac{C_e}{Oe}$ vs. C_e gives a straight line with;

Slope =
$$\frac{1}{Q_{m1}}$$
 and intercept = $\frac{1}{Q_{m1}K_{L1}}$ for

Langmuir-type 1.

$$\frac{1}{Q_e} = \frac{1}{Qm2} + \left(\frac{1}{K_{L2}q_{m2}}\right) \frac{1}{Ce}$$
 (5)

A plot of $\frac{1}{Q_e}$ vs. $\frac{1}{Ce}$ gives a straight line with;

Slope =
$$\frac{1}{K_{L2}Q_{m2}}$$
 and intercept = $\frac{1}{Qm2}$ for

Langmuir-type 2.

where Q_{mi} (mg/g) represents the Langmuir maximum monolayer adsorption capacity; K_{Li} is the Langmuir equilibrium constant (L/mg).

A dimensionless constant, S_L given in equation 6, known as the separation factor [29] is used to determine the nature the adsorption process, which is the favourability of sorption [18]. When $0 < S_L < 1$, the sorption is described as favourable.

$$S_L = \frac{1}{1 + K_L Co} \tag{6}$$

where K_L is the Langmuir equilibrium constant (L/mg).

(b) Freundlich isotherm

The Freundlich model is the earliest known relationship describing the non-ideal and reversible adsorption, which can be applied to multilayer adsorption, on the basis of an assumption concerning the energetic surface heterogeneity [30-31]. It is expressed in equation 7;

$$Q_e = K_f C_e^{1/n} \tag{7}$$

The linear transformed (LTF) model can be shown as equation 8;

$$ln Q_e = ln K_f + \frac{1}{n} ln C_e$$
 (8)

where, K_f (mg^{1-1/n}L^{1/n}g⁻¹) is an indicator of the sorption capacity; n gives an indication of the favourability sorption [28, 32].

A plot of $\ln Q_e$ vs. $\ln C_e$ gives a straight line with slope =1/n and intercept $=\ln K_f$ [12], [32].

(c) Redlich-Peterson isotherm

The Redlich-Peterson isotherm incorporates elements from both Langmuir and Freundlich isotherms. Therefore, it is chosen to confirm the type of isotherm, especially in cases where the decision to choose which of the two models best described the sorption system is not straightforward [18]. It is expressed in equation 9;

$$Qe = \frac{K_R Ce}{1 + A_R C_e^{\beta}} \tag{9}$$

The LTF model can be expressed in equation 10;

$$ln (K_R \frac{Ce}{Qe} - 1) = lnA_R + \beta lnC_e$$
 (10)

where K_R (L/g) is the isotherm constant; A_R (L/mg) is also an isotherm constant and β is an exponent which lies between 0 to 1. When the value of β =1, equation 9 becomes the same as the Langmuir isotherm equation [12, 33].

The model parameters are obtained by a plot of $ln(K_R \frac{Ce}{Qe} - 1)$ vs. $ln C_e$ and employing trial and error linear regression by adjusting the value of K_R to obtain the highest possible value of (R^2) . This can be determined by minimizing the distance between the experimental data points and the theoretical model predictions with the *solver* add-in function of the Microsoft EXCEL [12].

ii. Nonlinear Regression Methods

Error functions were employed to evaluate the isotherm constants and compare them with LTF model values [12] due to the inherent bias of LTF models resulting from linearization, altering the error distribution structure of isotherm [29-30, 34]. A trial and error procedure, which is applicable to computer operation was employed to determine the isotherm parameters by minimizing the distance between experimental data and isotherm models using Microsoft Excel's *solver* add-in function [12, 35-37]. The error function with the lowest value is selected.

(a) Hybrid Fractional Error Function (HYBRID)

The HYBRID [38] is widely reported for the consistency of its values for comparisons [12, 39]. It improves the fit of the sum square of errors (*ERRSQ*) at low concentrations [12, 29]. The mathematical statement is given in equation 11;

$$HYBRID = \frac{100}{\varphi - \mu} \sum_{i=1}^{\varphi} \left[\frac{(Q_{e,m} - Q_{e,c})^2}{Q_{e,m}} \right]_i (11)$$

(b) Marquardt's Percent Standard Deviation (MPSD)

The Marquardt error function [40] is similar to geometric mean error distribution modified according to the number of degrees of freedom in the system [29-30, 38]. It is expressed in equation 12;

$$MPSD = 100 \left(\sqrt{\frac{1}{\varphi - \mu} \sum_{i=1}^{\varphi} \left[\frac{(Q_{e,m} - Q_{e,c})}{Q_{e,m}} \right]_{i}^{2}} \right) \quad (12)$$

where $Q_{e,m}$ is the measured equilibrium solid phase sorbate concentration; $Q_{e,c}$ is the calculated equilibrium solid phase sorbate concentration; μ represents the number of fitted parameters; φ represents the data points.

III. Results and DiscussionsA. Equilibrium Sorption Isotherms

The experimental results and sorption isotherms for both CSB600 and MCSB600 are presented in Tables 2-3 and Figure 2 respectively. Similar

pattern to the L-type of isotherm classification by [41] were obtained. This suggests that the adsorbents are able to adsorb the MB from the solution at lower concentrations due to availability of sorption sites within them before reaching the maximum capacities. A sudden drop was observed at the highest concentration of 32.70 mg/l indicating a possibility of saturation of all the sorption sites. [42] reported that vacant sorption sites are available during the initial stage of sorption, and after a certain period, the available sites get occupied by dye molecules and during saturation, a repulsive force is created between adsorbate on the adsorbent's surface and in bulk phase.

Table 2: Results of batch sorption experiment and isotherm for CSB600

Coa	Ce Ia	Ce IIa	Cea	Qe I ^b	Qe II ^b	Qe ^b	Ce/Qe	1/Qe	1/Ce	In Qe	In Ce	In $[K_R Ce/Qe-1]$
3.70	1.10	1.20	1.15	1.30	1.25	1.28	0.90	0.78	0.51	0.24	0.14	1.65
12.50	5.20	5.00	5.10	3.65	3.75	3.70	1.38	0.27	0.20	1.31	1.63	2.14
26.60	16.30	16.20	16.25	5.15	5.20	5.18	3.14	0.19	0.06	1.64	2.79	3.02
32.70	23.10	23.40	23.25	4.80	4.65	4.73	4.92	0.21	0.04	1.55	3.15	3.40

Table 3: Results of batch sorption experiment and isotherm for MCSB600

Coa	Ce I ^a	Ce IIa	Cea	Qe I ^b	Qe II ^b	Qe ^b	Ce/Qe	1/Qe	1/Ce	In Qe	In Ce	In [K _R Ce/Qe-1]
3.70	1.00	1.20	1.10	1.35	1.25	1.30	0.85	0.77	0.91	0.26	0.10	0.02
12.50	5.80	6.00	5.90	3.35	3.25	3.30	1.79	0.30	0.17	1.19	1.77	1.18
26.60	17.30	17.10	17.20	4.65	4.75	4.70	3.66	0.21	0.06	1.55	2.84	2.04
32.70	24.20	23.30	23.75	4.25	4.70	4.48	5.31	0.22	0.04	1.50	3.17	2.45

 $^{\rm a}$ mg/l $^{\rm b}$ mg/g

Model	Parameters	CSB600	MCSB600
	Q_m	5.590	5.229
	K_L	0.332	0.315
LANG-L1	R^2	0.9828	0.9928
	HYBRID	5.87	1.304
	Q_m	6.467	5.298
	K_L	0.215	0.295
LANG-L2	R^2	0.9942	0.9987
	HYBRID	6.23	1.154
	1/n	0.452	0.421
	K_f	1.373	1.345
FR-L	R^2	0.9015	0.9548
	HYBRID	21.69	8.632
	A_R	4.252	0.851
	β	0.600	0.800
RP-L	K_R	6.887	2.383
	R^2	0.9392	0.9930
	HYBRID	37.37	5.931

Table 4: Isotherm parameters for CSB600 and MCSB600 obtained using linear regression

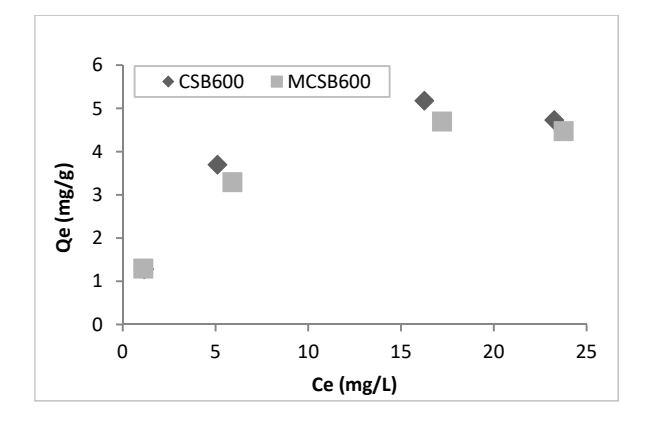


Figure 2: Isotherm on the sorption of MB on CSB600 and MCSB600 respectively.
3.2 Linear Regression

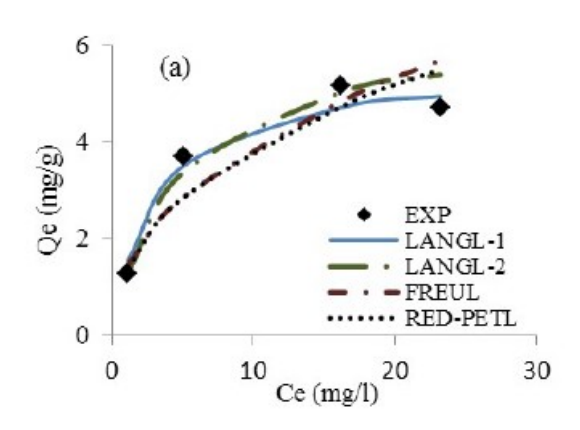
B. Linear Regression

The isotherm parameters obtained through linear regression methods by the plots of LTF of Langmuir (LANG-L1 and LANG-L2), Freundlich (FR-L) and Redlich-Peterson (RP-L) respectively are presented in Table 4. The parameters were used to generate the predicted isotherms which are compared against the experimental isotherms for descriptions of the sorption system are presented in Figure 3.

High R^2 values were obtained ranging from 0.9015 to 0.9987. The Langmuir provided the

best fitted model for the sorption systems across the two sorbents as presented in Table 1 due to higher the R^2 values.

Specifically, the LANG-L2 provided a better fit compared to the LANG-L1 model. The models followed the order LANG-L2 > LANG-L1 > RP-L > FR-L for CSB600 and LANG-L2 > RP-L > LANG-L1 > FR-L for MCSB600. The *HYBRID* also confirmed the LANG isotherm to be best fitted which follows the order, LANG-L1 > LANG-L2 > FR-L > RP-L for CSB600 and LANG-L2 > LANG-L1 > RP-L > FR-L for MCSB600.



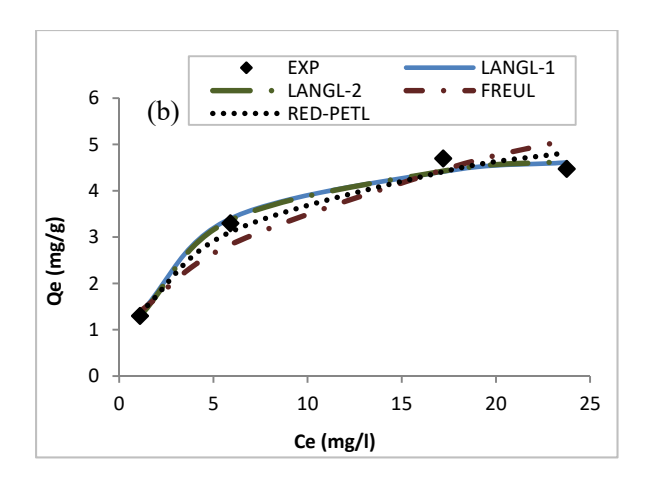


Figure 3: Predicted isotherms compared with experimental isotherms for (a) CSB600 and (b) MCSB600.

The maximum monolayer adsorption capacity, Q_m across the two sorbents were similar to the highest obtained experimental equilibrium sorption capacities, Q_e which makes the Q_m easier to be compared directly to Q_e . This is an advantage over the Freundlich sorption capacity, K_f because its implicit unit is difficult to convert [43]. Both Q_m and K_f of the adsorbents are in the same order of CSB600 > MCSB600. The reciprocal of 1/n gives the exponent, n. It is related to the energetic heterogeneity of the adsorbent surface [43].

The *n* values were 2.21 and 2.37, therefore, the sorption are favourable for both CSB600 and MCSB600 respectively. This implies possibility of sorption by the sorbents at low initial concentrations [43]. The Langmuir's S_L as shown in Figure 4 ranged from 0.09 to 0.55, indicating also a favourable sorption process.

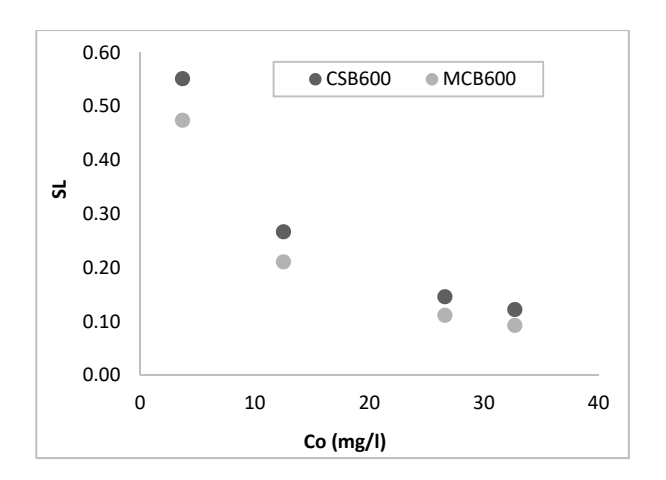


Figure 4: Relationship between Langmuir separation factor and the initial concentration.

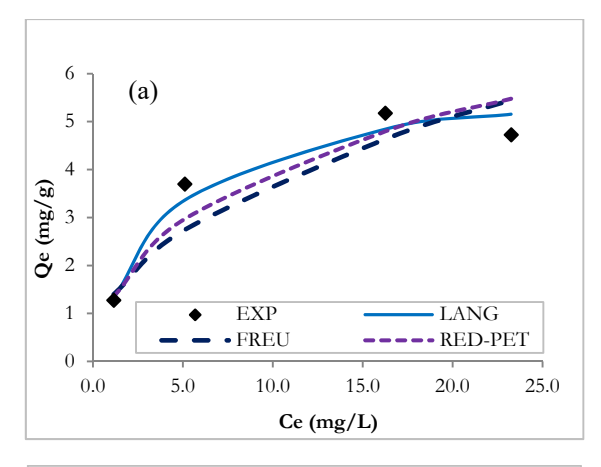
The favourability of sorption increases as the initial concentration increases across all the sorbents. However, it was observed that sorption of MB was more favourable at higher initial concentrations. MCSB600 had a more favourable sorption due to lower S_L values compared to CSB600.

C. Nonlinear Regression

The Langmuir model again proved to be the best fit from both the *HYBRID* and *MPSD* error functions. Nevertheless, *HYBRID* proved the better fit compared to the *MPSD*. The isotherm models generated different parameters and are presented in Tables 5 and 6.

Table 5: Isotherm parameters obtained for CSB600 using error functions by nonlinear regression method

Isotherm	Parameters	MPSD	HYBRID
LANG	Q_m	6.06	5.81
	K_L	0.244	0.290
	$R^{\frac{1}{2}}$	0.9563	0.9638
	ERROR	10.61	4.58
FREUN	K_f	1.310	1.490
	1/n	0.452	0.407
	R^2	0.8382	0.8496
	ERROR	23.52	13.52
RED-PET	K_R	2.645	1.593
	A_R	0.134	0.268
	β	0.699	1.000
	R^2	0.8818	0.9606
	ERROR	27.07	8.75



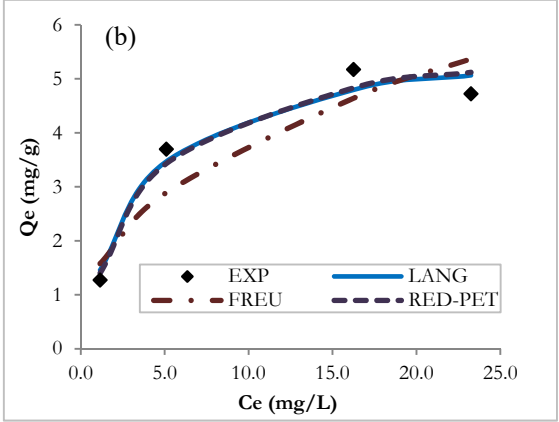
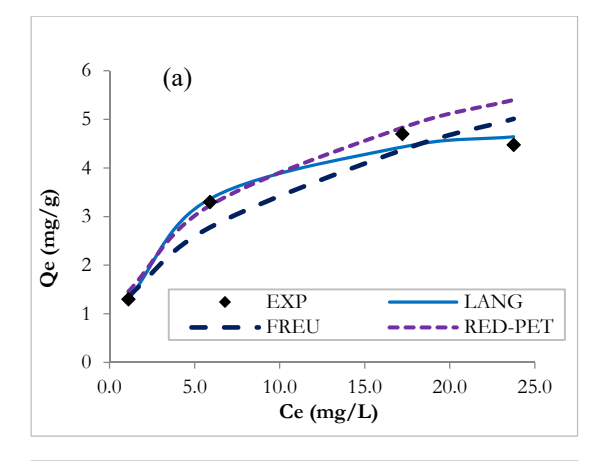


Figure 5: Experimental and predicted isotherms of CSB600 using (a) MPSD and (b) HYBRID.

Table 6: Isotherm parameters obtained for MCSB600 using error functions by nonlinear regression method

Isotherm	Parameters	MPSD	HYBRID
LANG	Q_m	5.31	5.33
	K_L	0.293	0.29
	R^2	0.9857	0.9857
	ERROR	5.04	1.145
FREUN	K_f	1.31	1.428
	1/n	0.423	0.391
	R^2	0.9188	15.20
	ERROR	15.27	7.871
RED-PET	K_R	3.600	1.547
	A_R	1.603	0.290
	β	0.702	1.000
	R^2	0.9477	24.29
	ERROR	24.29	2.290



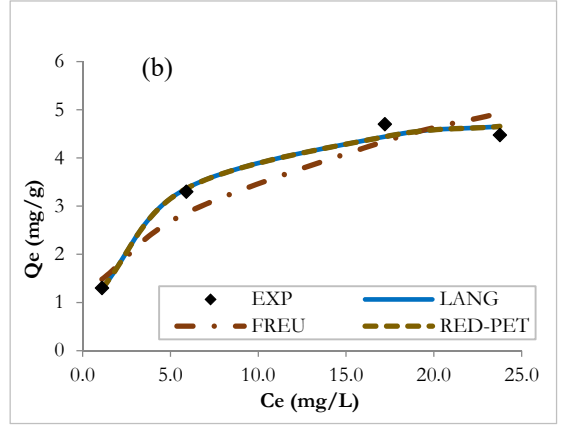


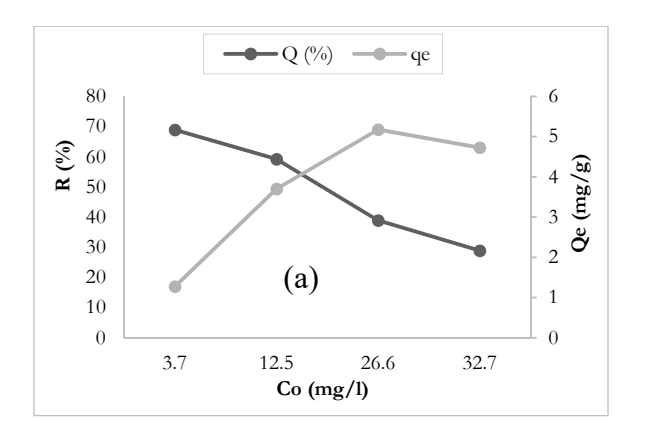
Figure 6: Experimental and predicted isotherms of MCSB600 using (a) MPSD and (b) HYBRID.

The HYBRID proved the sorption process to be a special case of Langmuir isotherm as the Redlich-Peterson's adsorption affinity, β was observed to be one (1) across both CSB600 and MCSB600. The Redlich-Peterson's isotherm overlaps the Langmuir across both the sorbents from the comparison of the predicted against the experimental isotherms in Figure 5(b) and 6(b).

D Effect of Initial MB Concentration on Adsorption

The adsorption efficiency, R decreased with increasing initial concentration while the sorption capacity, Q_e increased with initial concentration. The adsorption efficiencies are such that CSB600 had higher sorption efficiencies than MCSB600. A sudden decrease

in Q_e was observed at the highest initial concentration conforming to the assertion on saturation of the available sorption sites. The relationship between removal efficiency, equilibrium capacity and initial concentration are presented in Figure 7. Similar results were obtained by [5], and it was attributed that at lower concentration, the ratio of the initial number of MB molecules to the available surface area is low.



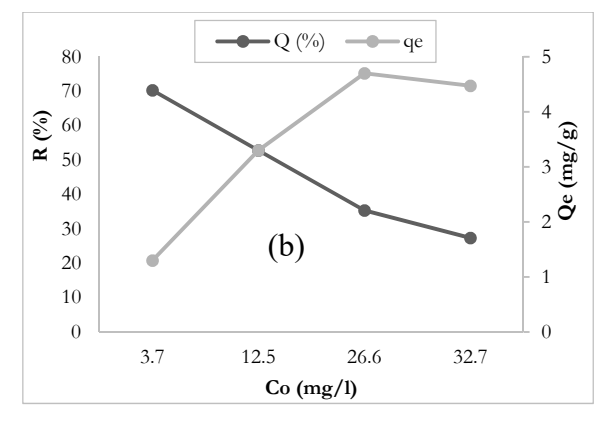


Figure 7: Effect of initial concentration on sorption of MB in (a) CSB600 and (b) MCSB600.

IV. Conclusion

The adsorption behaviour of both CSB600 and MCSB600 was described by Langmuir isotherm with sorption capacities of 5.59 and 5.23 mg/g respectively. The sorption capacity of MCSB600 reduced by only 6.46% from its precursor

(CSB600). Also, Magnetisation did not affect the sorption performance of MB as the isotherms were similar (p-value = 0.088). This suggests magnetised biochar has a promising future for the adsorption of aqueous MB solution.

References

- [1] Isah, U.A., Giwa, A., Bala, S., Muhammad, S. and Abdullahi, M. Kinetics equilibrium and thermodynamics studies of C.I. reactive blue 19 dye adsorption on coconut shell based activated carbon, *International Biodeterioration and Biodegradation*, 2015, pp.1–9. https://doi.org/10.1016/j.ibiod.2015.04.006
- [2] Mathew, M., Desmond, R.D. and Caxton, M. "Adsorption of Methylene Blue from Aqueous Solutions Using Biochar Prepared from Eichhorrnia Crassipes (Water Hyacinth)-Molasses Composite: Kinetic and Equilibrium Studies", African Journal of Pure and Applied Chemistry, Vol. 10, No.6, 2015, pp. 63-72. https://doi.org/10.5897/AJPAC2016.0703
- [3] Dakhil, I.H. "Adsorption of Methylene Blue Dye from Wastewater by Spent Tea Leaves", Journal of Kerbala University, Vol.11, No.3, 2016.
- [4] Juang, R., Yei, Y., Liao, C., Lin, K., and Lu, H. "Synthesis of Magnetic Fe₃O₄/Activated Carbon Nanocomposites With High Surface Area As Recoverable Adsorbents", *Journal of the Taiwan Institute of Chemical Engineers*, 000, ,2018, pp. 1–10. https://doi.org/10.1016/j.jtice.2017.12.005
- [5] Khodaie, M., Ghasemi, N., Moradi, B., and Rahimi, M. "Adsorption of Methylene Blue From Wastewater By Adsorption unto Zncl₂ Activated Corn Husk Carbon Equilibrium Studies", *Journal of Chemistry*, 2013.
- [6] Santhi, M., Kumar, P.E., and Muralidharan, B. "Adsorption of Malachite Green Dyes by Adsorption Onto Activated Aarbon–Mno₂– Nanocomposite: Kinetic Study and Equilibrium Isotherm Analyses", *IOSR Journal of Applied Chemistry*, Vol. 8, No.4, 2015, pp. 33–41. https://doi.org/10.9790/5736-08413341
- [7] Ruthiraan, M., Abdullah, E. C., Mubarak, N. M., and Nizamuddin, S. "Adsorptive Adsorption Of Methylene Blue using Magnetic Biochar Derived from Agricultural Waste Biomass: Equilibrium, Isotherm, Kinetic Study",

- International Journal of Nanoscience, Vol.17, No.5, 2018, pp.1–12. https://doi.org/10.1142/S0219581X18500023
- [8] Rahman, M.A., Amin, S. M.R., and Alam, A. M.S. . "Adsorption of Methylene Blue From Wastewater Using Activated Carbon Prepared From Rice Husk", *Dhaka Univ. J. Sci.*, Vol. 60, No. 2,2012, pp.185–189
- [9] Kargi, F., and Ozmihci, S. (2004). "Biosorption performance of powdered activated sludge for adsorption of different dyestuffs", Enzyme and Microbial Technology, 35, 267–271. https://doi.org/10.1016/j.enzmictec.2004.05.0 02.
- [10] Oladipo, M.A., Bello, I.A., Adeoye, D.O., Abdulsalam, K. A., and Giwa, A.A. "Sorptive Adsorption of Dyes From Aqueous Solution: A Review", *Advances in Environmental Biology*, Vol. 7, No.11,2013, pp. 3311–3327.
- [11] Jiang, T., Liang, Y., He, Y., and Wang, Q. "Activated Carbon/NiFe₂O₄ Magnetic Composite: A Magnetic Adsorbent for The Adsorption Of Methyl Orange", *Journal of Environmental Chemical Engineering*, 2015. https://doi.org/10.1016/j.jece.2015.06.020
- [12] Wong, Y. C., Szeto, Y. S., Cheung, W. H., and Mckay, G. "Adsorption Of Acid Dyes On Chitosan-Equilibrium Isotherm Analyses", *Process Biochemeistry*, Vol. *39*, 2004,pp.693–702. https://doi.org/10.1016/S0032-9592(03)00152-3
- [13] Babaei, A. A., Alavi, S. N., Akbarifar, M., Ahmadi, K., Esfahani, A. R., and Kakavandi, B. "Experimental And Modeling Study on Adsorption of Cationic Methylene Blue Dye Onto Mesoporous Biochars Prepared from Agrowaste", *Desalination and Water Treatment*, 2016, 3994. https://doi.org/10.1080/19443994.2016.1163 736
- [14] PubChem (2013). "Methylene Blue", PubChem database. National Center for Biotechnplogy Information. Retrieved from: https://pubchem.ncbi.nlm.nih.gov/ online database.
- [15] Bordoloi, N., Dey, M.D., Mukhopadhyay, R., and Kataki, R. (2017). "Adsorption of Methylene Blue and Rhodamine B By Using Biochar Derived From Pongamia Glabra Seed Cover", Water Science and Technology, 2017. https://doi.org/10.2166/wst.2017.579

- [16] Berrios, M., Martin, M., and Martin, A. "Adsorption of Methylene Blue Onto Olive-Based Activated Carbon", *Journal of Industrial and Engineering Chemistry*, Vol. 18, 2012, pp.780–784. https://doi.org/10.1016/j.jiec.2011.11.125
- [17] Han, Z., Sani, B., Mrozik, W., Obst, M., Beckingham, B., Karapanagioti, H. K., and Werner, D. "Magnetite Impregnation Effects on the Sorbent Properties of Activated Carbons and Biochars", Water Research, 70,2014, pp.394– 403.
- https://doi.org/10.1016/j.watres.2014.12.016
- [18] Sani, B. S. "Modelling of Pollutant Adsorption by Activated Carbon and Biochar With and Without Magnetite Impregnation for The Treatment of Refinery annd other Wastewaters", *Doctoral thesis, Newcastle University.* 2017 Retrieved from https://thesis.ncl.ac.uk/dspace/bitstream/104 43/3595/1/Sani%2C B.S. 2017.pdf.
- [19] Mohan, D., Sarswat, A., Singh, V. K., Alexandre-Franco, M., and Pittman Jr., C. U. (2011). "Development of Magnetic Activated Carbon from Almond Shells for Trinitrophenol Removal from Water", *Chemical Engineering Journal*, Vol.172, No. 2–3,2011, pp.1111–1125. https://doi.org/10.1016/j.cej.2011.06.054
- [20] Safarik, I., Nymburska, K., and Safarikova, M. "Adsorption of Water-Soluble Organic Dyes on Magnetic Charcoal", *Journal Chemical Technology* and Biotechnology, Vol. 69,1997, pp. 1–4
- [21] Zhang, G., Qu, J., Liu, H., Cooper, A. T., and Wu, R. "Cufe₂O₄/Activated Carbon Composite: A Novel Magnetic Adsorbent for the Adsorption of Acid Orange II and Catalytic Regeneration", *Chemosphere*, Vol. 68, 2007, pp. 1058–1066. https://doi.org/10.1016/j.chemosphere.2007. 01.081
- [22] Castro, C. S., Guerreiro, M. C., Goncalves, M., Oliveira, L. C. A., & Anastácio, A. S. (2009). "Activated Carbon/Iron Oxide Composites For The Adsorption Of Atrazine From Aqueous Medium", *Journal of Hazardous Materials*, Vol. 164, 2009, pp. 609–614. https://doi.org/10.1016/j.jhazmat.2008.08.066
- [23] Mohan, D., Sarswat, A., Singh, V.K., Alexandre-Franco, M., and Pittman Jr., C.U. (2011). "Development of Magnetic Activated Carbon From Almond Shells for Trinitrophenol Adsorption from Water", Chemical Engineering

- Journal, Vol. 172, No. 2–3, pp.1111–1125. https://doi.org/10.1016/j.cej.2011.06.054
- [24] Choi, Y., Wu, Y., Sani, B., Luthy, R. G., Werner, D., and Kim, E. "Performance of Retrievable Activated Carbons То Treat Sediment Contaminated with Polycyclic Aromatic Hydrocarbons", Journal of Hazardous Materials, pp.359-367. Vol. 320, 2016, https://doi.org/10.1016/j.jhazmat.2016.08.047
- [25] Han, Z., Badruddeen, S., Akkanen, J., Abel, S., Nybom, I., Karapanagioti, H. K., & Werner, D. "A Critical Evaluation of Magnetic Activated Carbon's Potential for the Remediation of Sediment Impacted by Polycyclic Aromatic Hydrocarbons". *Journal of Hazardous Materials*, (December), 2016,pp.41–47. https://doi.org/10.1016/j.jhazmat.2014.12.030
- [26] Mubarak, N.M., Fo, Y.T., & Al-salim, H.S. "Adsorption of Methylene Blue and Orange-G from Wastewater using Magnetic Biochar", Vol.14, No,4, 2015, pp.1–13. https://doi.org/10.1142/S0219581X1550009 X
- [27] Langmuir, I. "The Constitution and Fundamental Properties of Solids and Liquids", Vol. 468, No.15, 1916, Met. Chem. Eng.
- [28] Mc Kay, G., Blair, H. S., and Gardner, J. "Rate Studies for the Adsorption of Dyestuffs Onto Chitin", *Journal of Colloid and Interface Science*, Vol. 95, No.1, 1983
- [29] Ayawei, N., Ebelegi, A. N., and Wankasi, D. "Modelling and Interpretation of Adsorption Isotherms", *Journal of Chemistry*. 2017
- [30] Foo, K. Y., and Hameed, B. H. "Insights into the Modeling of Adsorption Isotherm Systems", *Chemical Engineering Journal Journal*, Vol. 156, 2010, pp.2–10. https://doi.org/10.1016/j.cej.2009.09.013
- [31] Chen, X. "Modeling of Experimental Adsorption Isotherm Data", *Information*, Vol.6, 2015, pp.14–22. https://doi.org/10.3390/info6010014
- [32] Lonappan, L., Rouissi, T., Kumar, R., Brar, S. K., Avalos, A., Verma, M. and Valero, J. R. "Adsorption of Methylene Blue on Biochar Microparticles Derived From Different Waste Materials", Waste Management, 2016, pp. 1–8. https://doi.org/10.1016/j.wasman.2016.01.01
- [33] Wu, F., Liu, B., Wu, K., and Tseng, R. "A New

- Linear Form Analysis of Redlich-Peterson Isotherm Equation for the Adsorptions of Dyes", *Chemical Engineering Journal*, Vol. 162, No.1, 2010, pp. 21–27. https://doi.org/10.1016/j.cej.2010.03.006
- [34] Kumar, K. V., Porkodi, K., and Rocha, F. "Isotherms and Thermodynamics by Linear and Non-Linear Regression Analysis for the Sorption of Methylene Blue onto Activated Carbon: Comparison of Various Error Functions", *Journal of Hazardous Materials*, Vol. 151, 2008, pp. 794–804. https://doi.org/10.1016/j.jhazmat.2007.06.056
- [35] Ho, Y., Chiu, W.-T., and Wang, C.C. "Regression Analysis for the Sorption Isotherms of Basic Dyes on Sugarcane Dust", *Bioresource Technology*, Vol. 96, 2005, pp. 1285–1291. https://doi.org/10.1016/j.biortech.2004.10.02
- [36] Kumar, K.V., and Sivanesan, S. "Comparison of Linear and Non-Linear Method in Estimating the Sorption Isotherm Parameters for Safranin onto Activated Carbon", *Journal of Hazardous Materials*, Vol. 123, 2005, pp. 288–292. https://doi.org/10.1016/j.jhazmat.2005.03.040
- [37] Salarirad, M.M., and Behnamfard, A. "Modelling of Equilibrium Data for Free Cyanide Adsorption onto Activated Carbon by Linear and Non-Linear Regression Methods", 2011 International Conference on Environment and Industrial Innovation, Vol. 12, 2011, pp. 79–84.
- [38] Porter, J.F., Mckay, G., and Choy, K. H. "The Prediction of Sorption from A Binary Mixture of Acidic Dyes Using Single-and Mixed-Isotherm Variants of the Ideal Adsorbed Solute Theory", *Chemical Enginnering Science*, Vol. 54, 1999, pp.5863–5885.
- [39] Boulinguiez, B., Cloirec, P. Le, and Wolbert, D. (2008). "Revisiting the Determination of Langmuir Parameters-Application to Tetrahydrothiophene Adsorption onto Activated Carbon", *Langmuir*, Vol. 24, No. 5, 2008, pp. 6420–6424.
- [40] Marquardt, D. W. "An Algorithm for Least-Squares Estimation of Nonlinear Parameters", Journal of Society of Applied Mathematics, Vol. 11, No.2, 1963.
- [41] Limousin, G., Gaudet, J.P., Charlet, L., Barthes, V., and Krimissa, M. "Sorption Isotherms: A Review on Physical Bases , Modeling and

- Measurement", *Applied Geochemistry*, Vol. 22, 2007, pp. 249–275. https://doi.org/10.1016/j.apgeochem.2006.09. 010
- [42] Banerjee, S., and Chattopadhyaya, M.C. "Adsorption Characteristics For The Adsorption of a Toxic Dye, Tartrazine from Aqueous Solutions by a Low Cost Agricultural By-Product", *Arabian Journal of Chemistry.* 2013. https://doi.org/10.1016/j.arabjc.2013.06.005
- [43] Worch, E. Adsorption technology in water treatment: fundamentals, processes, and modelling, De Gruyter, 2012